JOURNAL OF MATERIALS SCIENCE 19 (1984) 327–338

Radiation damage and high resolution electron microscopy of polydiacetylene crystals

R. T. READ, R. J. YOUNG
Department of Materials, Queen Mary College, Mile End Road, London E1 4NS, UK

The relationship between radiation damage and the application of high resolution electron microscopy (HREM) to polydiacetylene single crystals has been examined. The damage is seen to occur by the decay of electron diffraction patterns and the loss of contrast in bright- and dark-field micrographs. The rate of damage was found to be different for the two polydiacetylene derivatives studied and to take place probably by cross-linking. It was found that lattice images from planes parallel to the chain direction with a spacing of 0.9 ± 0.1 nm could be obtained from the most resistant derivative. Images of chain-end dislocations were obtained for the first time in a polymer crystal. The problems of applying HREM to polymers and the conditions for imaging individual molecules are discussed.

1. Introduction

High resolution electron microscopy (HREM) is now becoming an important method of determining the organization of molecules and atoms in crystals and in particular the detailed structure of interfaces and defects. The technique has been applied with considerable success to the study of intermetallic compounds [1] and metallic carbides [2] and oxides [3] and, most recently metals [4], but attempts to use HREM for the study of organic molecules [5–9] and polymers [10–14] have proved more difficult. The main problem is that organic molecules suffer radiation damage in the electron beam during examination in the electron microscope and this severely limits the resolution that can be attained. The problem of radiation damage has been reviewed by Grubb [15], Glaeser [16], Zeitler [17] and Jones [18]. For a particular type of organic material successful electron microscopy has necessitated the use of high accelerating voltages [9, 18–20], low temperatures [18, 19], sensitive photographic film and skillful and rapid operation of the microscope. The problem of radiation damage is particularly acute in the application of HREM to polymers because of the high magnifications employed and the corresponding high intensity of radiation that is used with this technique. However, there is a need for more information upon the structure of defects in polymer crystals and this paper is concerned with the behaviour of two polydiacetylenes, one of which has proved to be particularly resistant to radiation damage and allowed a detailed study of its structure using HREM.

It is well known that chemical modification of organic materials can significantly reduce radiation damage. For example, Fryer [21] and Uyeda and co-workers [22] have shown that chlorination of copper phthalocyanin can increase the electron beam stability of the material by up to a factor of 30 over the patent material. In conventional polymers stabilization has been achieved by introducing a ring structure into the polymer backbone. Lamellar single crystals of poly (*p*-xylylene) were used by Keller [10] to obtain lattice images and by Tsuji and co-workers [14] to obtain molecular images. These results reflected a quoted [14] 20-fold increase in stability over the most widely-studied crystalline polymer, polyethylene. Because of the chain-folded conformations of the molecules in these lamellar crystals the beam direction is approximately parallel to the molecular axes and

0022–2461/84 $03.00 + .12

so the molecules can only be viewed "end-on". This problem can be overcome to a certain extent by using specimens in which the molecules are in extended conformations. For example, lattice images from planes parallel to the chain direction have been obtained by Dobb and co-workers [11] from sections of aromatic polyamide fibres (Kevlar 49) indicating that this polymer has considerable resistance to radiation damage. Also Thomas and co-workers [12] have obtained lattice images from poly (*p*-phenylene benzobisthiazole) fibres which appear to be even more resistant to radiation damage than Kevlar. However, both of these types of fibres are polycrystalline and the crystalline regions relatively small (~ 20–80 nm). Hence lattice planes can only be resolved over relatively small regions.

Recently we have reported [13] that it is possible to image large areas of the crystal lattice in certain polydiacetylene single crystals. These crystals are 100% crystalline with a ribbon-like morphology and the molecules are oriented such that they lie parallel to the ribbon axis. This means that they can be viewed with the electron beam perpendicular to the chain direction in the electron microscope. Other studies [23, 24] have shown that crystals of other diacetylene polymer derivatives contain defects such as stacking faults [23] and dislocations [24] and it is the purpose of this present study to examine the radiation sensitivity of different polydiacetylene single crystals and to show how this affects the ability to obtain lattice images and images of defects in these materials.

2. Experimental details

2.1. Specimen preparation

Two particular polydiacetylenes were studied with the chemical formulae:

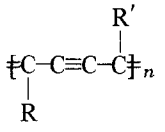

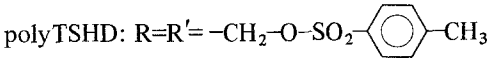

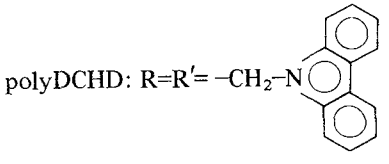

The poly TSHD was prepared by allowing a few drops of a 10^{-2} M monomer solution in xylene to evaporate on the surface of water. This produced thin (~ 100 nm) lamellar crystals which were collected using copper grids. The crystals were subsequently polymerized by heating for ~ 24 h at 80° C [25].

The poly DCHD was prepared in two different ways as it tended to form ribbon-like fibres rather than lamellar crystals from most solvents. For the radiation damage measurements a few drops of 10^{-3} M monomer solution were applied to a carbon film on a copper grid and allowing the xylene solvent to evaporate. The crystals were then polymerized by heating for 24 h at 150° C [26]. In order to prepare very thin crystals (~ 20 nm) for HREM an alternative method of preparation was employed in this case. Monomer crystals were prepared by spraying a 4×10^{-3} M monomer solution in xylene onto {1 0 0} faces of freshly cleaved NaCl crystals. Evaporation of the fine droplets produced very small crystals which were polymerized on the NaCl for ~ 24 h at 150° C, coated with carbon and then collected by dissolving the NaCl in distilled water.

2.2. Radiation damage measurements

These measurements were carried out on a Jeol 100 CX transmission electron microscope using a Keithley 610 electrometer to monitor the beam intensity. The electrometer was connected to the output from the screen exposure monitor and this was calibrated using a specimen holder containing a Faraday cage. The technique has been described by Falls and Thomas [27] and the efficiency of the screen exposure monitor was found to be 63.3% at 100 kV. The radiation damage was monitored by following the decay of electron diffraction patterns. Specimens were exposed to a constant beam current and diffraction patterns were obtained at intervals, the "end-point" being judged as the radiation dose for complete disappearance of the diffraction pattern. The dose of radiation was determined from the beam current, the time of exposure and the size of the area selected for the diffraction pattern.

The poly TSHD crystals were found to be relatively sensitive to radiation and a beam current of 7×10^{-13} A was used. For the more resistant poly DCHD crystals a higher current of 5×10^{-11} A was used initially and this was increased in steps to 6×10^{-10} A towards the end of the run.

2.3. High resolution electron microscopy

The electron microscopes used were a Jeol 100 CX (side entry goniometer, $C_s = 2.8$ mm) and a Jeol 100 C (top entry goniometer, $C_s = 0.77$ mm), both operated at 100 kV. The instruments were carefully aligned using a small (200 μm) condenser aperture. The objective astigmatism was carefully adjusted at a magnification of 250 000 using a carbon film as described by several workers [28, 29]. In order to avoid radiation damage during focusing and microscope adjustment a minimal exposure technique was developed. The method used is similar to that employed by Williams and Fisher [30] and involved focusing on an area near to the area of interest, deflecting the beam temporarily, moving to the area of interest and then making the exposure. Image drift was overcome by using relatively short exposure times (~ 3 sec). This was facilitated by operating at 100 000 times magnification, focusing the condenser lens and using high-speed X-ray film (Industrex CX) with a grain size of approximately 5 μm. The dose of radiation necessary to obtain a useful micrograph was estimated to be about 2200 Cm^{-2}. An electron diffraction pattern involving a negligible dose of radiation was always obtained, using a defocused condenser lens, from the area of interest before micrographs were obtained. As far as possible, a series of micrographs were taken at different levels of defocus in order to obtain maximum contrast. Scherzer focus [21] was -125 nm for the 100 CX microscope and -62 nm for 100 C.

Although the resolution of the 100 C microscope used is better than that of the 100 CX similar results were obtained on the two instruments. This is because the resolution was limited by radiation damage in the material rather than by instrumental factors.

3. Results

3.1. Radiation damage

The radiation damage was monitored by observing the fading of spots in selected area diffraction patterns (SADP's) whilst carefully measuring the dose of radiation. For both types of polymer the crystals are oriented with their chain directions parallel to the support film and so approximately perpendicular to the electron beam. The crystal structures of both poly TSHD and poly DCHD are known to a high degree of accuracy and are given in Table I. Note that the chain direction has been indexed as c.

TABLE I Crystal structures of polydiacetylene single crystals. The structures have been indexed with the chain direction as c

Polymer	Poly TSHD [31]	Poly DCHD [32]
Space group	$P2_1/a$	$P2_1/a$
a (nm)	1.494	1.740
b (nm)	1.449	1.287
c (nm)	0.491	0.491
γ	118.1°	108.3°

3.3.1. Poly TSHD

Fig. 1 gives a series of [1 2 1] SADP's for a poly TSHD crystal, each micrograph being obtained from the same area of crystal after different lengths of time corresponding to increasing doses of radiation. The radiation damage is manifest first of all as the fading of the outer spots in the diffraction pattern. As the damage increases spots closer to the main beam start to disappear until eventually all that remains is a diffuse ring. This behaviour is expressed quantitatively in Fig. 2 where the lattice spacings of diffraction spots are plotted against the logarithm of the dose required to cause the spots to disappear. From measuring over 20 series of SADP's for poly TSHD crystals the "end-point" dose was found to be 104 ± 5 Cm^{-2}, which happens to be very similar to the value of 105 Cm^{-2} (Table II) quoted by Grubb and Groves for polyethylene [19]. The diffraction patterns obtained from poly TSHD faded gradually from the outside inwards but with no tendency for reflections from any particular orientations to persist longer than others. The radiation damage was also accompanied by a loss of contrast in bright and dark-field images.

3.1.2. Poly DCHD

Crystals of poly DCHD were found to be very much more stable than poly TSHD crystals and the radiation damage was also found to be dependent upon the orientation of the crystals on the substrate. Fig. 3 shows a series of [1 $\bar{1}$ 0] SADP's for a poly DCHD crystal. As with poly TSHD the pattern fades from the outside inwards, but in this case the dose required for complete loss of the pattern is over an order of magnitude greater. Again, the damage was accompanied by a loss of contrast in bright-field images. The effect of crystal orientation can be seen in Fig. 4 where a series of [1 2 2] patterns are given for increasing doses. After a dose of 2400 Cm^{-2} the spots on the first-

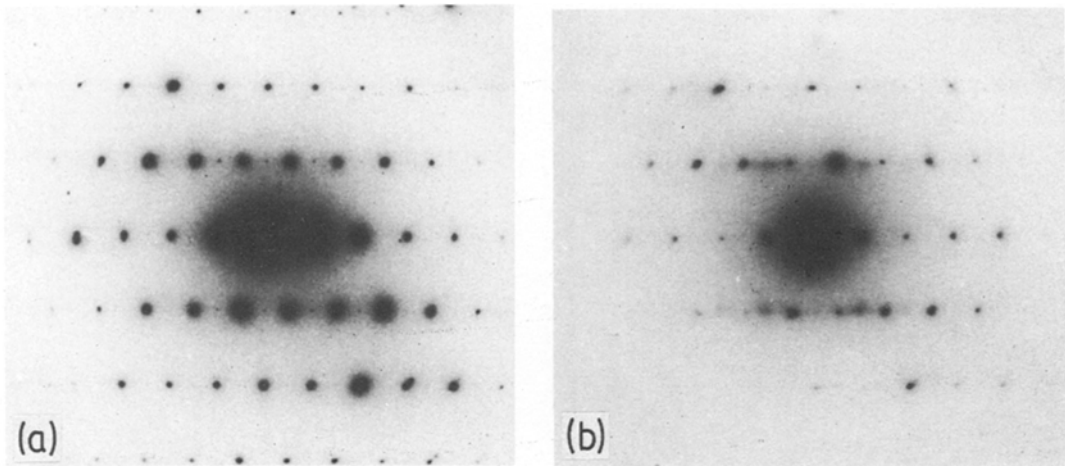

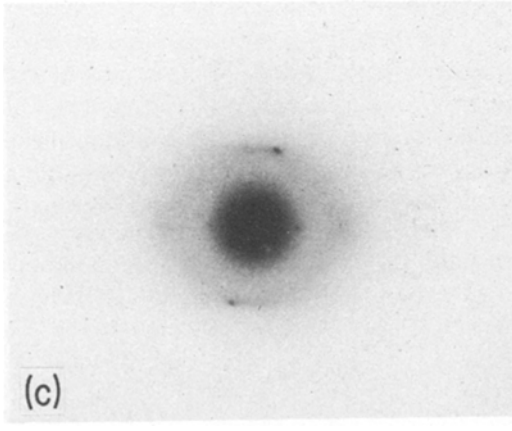

Figure 1 [1 2 1] SADP's from a poly TSHD crystal exposed to an increasing dose of radiation. (a) Dose–0 Cm^{-2}. (b) Dose–48 Cm^{-2}. (c) Dose–73 Cm^{-2}.

order layer lines have virtually disappeared but the $(2\,\bar{1}\,0)$ reflections upon the zero-order are still strong. These equatorial $(2\,\bar{1}\,0)$ reflections persist up to a dose of over 68 000 Cm^{-2} (Fig. 4c) and eventually disappear after a dose of the order of 200 000 Cm^{-2}. This behaviour was found to be very reproducible and so two "end-points" are quoted for poly DCHD in Table II, one for the first-order layer line reflections and the other for the $(2\,\bar{1}\,0)$ reflections. The behaviour is also shown graphically in Fig. 5. It is obvious from these results that poly DCHD is very much more stable than poly TSHD and polyethylene [19].

3.2. Change in lattice spacings

It was found that there was a small but consistent change in the lattice spacings in the polydiacetylene single crystals during exposure of the electron beam. Two types of planes were monitored, the layer line spacing corresponding to the chain direction repeat, c and the change in the spacing of $(2\,\bar{1}\,0)$ planes parallel to the chain direction.

3.2.1. Poly TSHD

The variation in the chain direction repeat, c and the spacing of $(2\,\bar{1}\,0)$ planes in poly TSHD with radiation dose is shown in Fig. 6. It can be seen that there is a small decrease in the c repeat from 0.49 nm to below 0.46 nm. On the other hand, within the limits of experimental error the $(2\,\bar{1}\,0)$ spacing does not change.

3.2.2. Poly DCHD

The variation in chain direction repeat, c and the spacing of the $(2\,\bar{1}\,0)$ planes for poly DCHD is

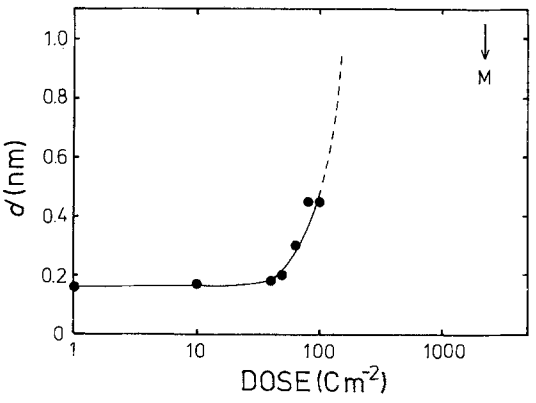

Figure 2 Dependence of d-spacings of fading diffraction spots upon radiation dose for poly TSHD. (The arrow indicates the dose required to obtain a micrograph).

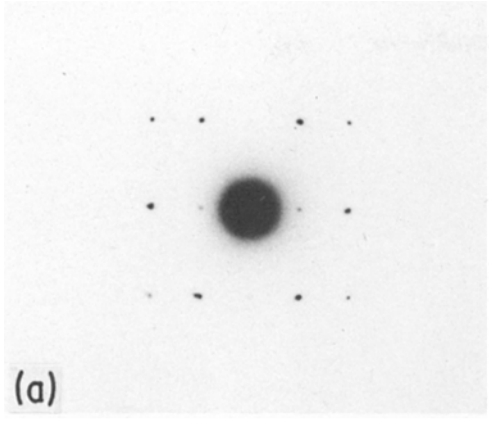

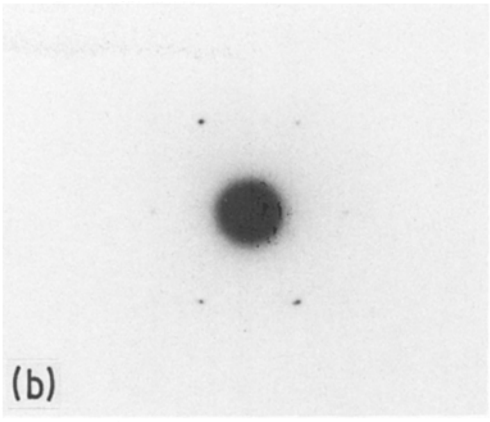

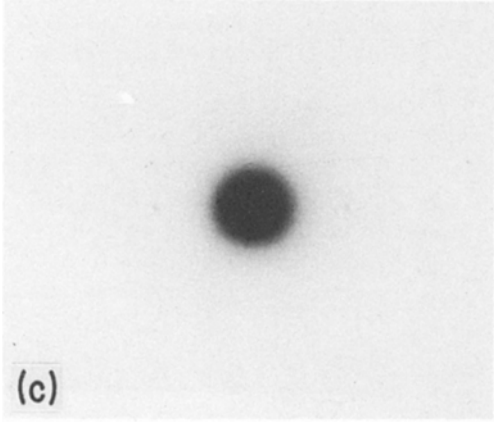

Figure 3 [1 $\bar{1}$ 0] SADP's from a poly DCHD crystal exposed to an increasing dose of radiation. (a) Dose–0 Cm^{-2}. (b) Dose–1400 Cm^{-2}. (c) Dose–1880 Cm^{-2}.

shown in Fig. 7. The layer line disappears relatively rapidly and it can be seen that there is a small decrease in the c repeat as for poly TSHD. The (2 $\bar{1}$ 0) spots are very stable and remain until a very high dose of radiation. The change in their lattice spacing is rather complex. Up to a dose of about 10 000 Cm^{-2} the spacing increases whereas with radiation above this dose it decreases.

3.3. Lattice images

Lattice images were obtained from the poly DCHD crystals but all attempts to obtain them from poly TSHD failed. However, this is understandable since a dose of about 2200 Cm^{-2} was necessary to obtain a micrograph and this is well beyond the "end-point" for poly TSHD (100 Cm^{-2}) but less than the "end-points" for poly DCHD. So far, four distinct lattice spacings, all from ($h\,k\,0$) planes have been resolved as shown in Figs. 8 to 11. In each case the associated SADP obtained from the same area as the micrograph is given and all of the fringes are parallel to the chain direction. Fig. 8 shows relatively widely spaced fringes at about separation of about 1.5 ± 0.1 nm. They are not particularly well-defined and correspond to the spacing of (1 0 0) planes (1.65 nm) in poly DCHD. Fig. 9 shows fringes at 1.3 ± 0.1 nm which correspond to (0 1 0) planes (1.22 nm) in poly DCHD.

TABLE II Electron doses required for loss of specific diffraction information at room temperature for organic materials at 100 kV (after [18])

Material	Critical dose ($C\,m^{-1}$)	Critical dose (electrons nm^{-2})	Remarks	Reference
Anthracene	1 000	6 000	loss of all reflections	[18]
Paraffin	60	360	loss of 0.415 nm reflections	[18]
Polyethylene	105	630	loss of all reflections	[19]
Polyoxymethylene	100	600	loss of all reflections	[19]
Poly (*p*-xylylene)	5 000	30 000	loss of all reflections	[14]
PPT (Kevlar)	> 2 000	> 12 000	loss of 0.433 nm reflections	[11]
PBT fibres	> 16 000	> 100 000	loss of equatorial reflections	[12]
Poly TSHD	104	620	loss of all reflections	*
Poly DCHD	2 500	15 000	loss of azimuthal reflections	*
Poly DCHD	~ 200 000	~ 1 200 000	loss of equatorial (2 $\bar{1}$ 0) reflections	*

*Results of this present study.

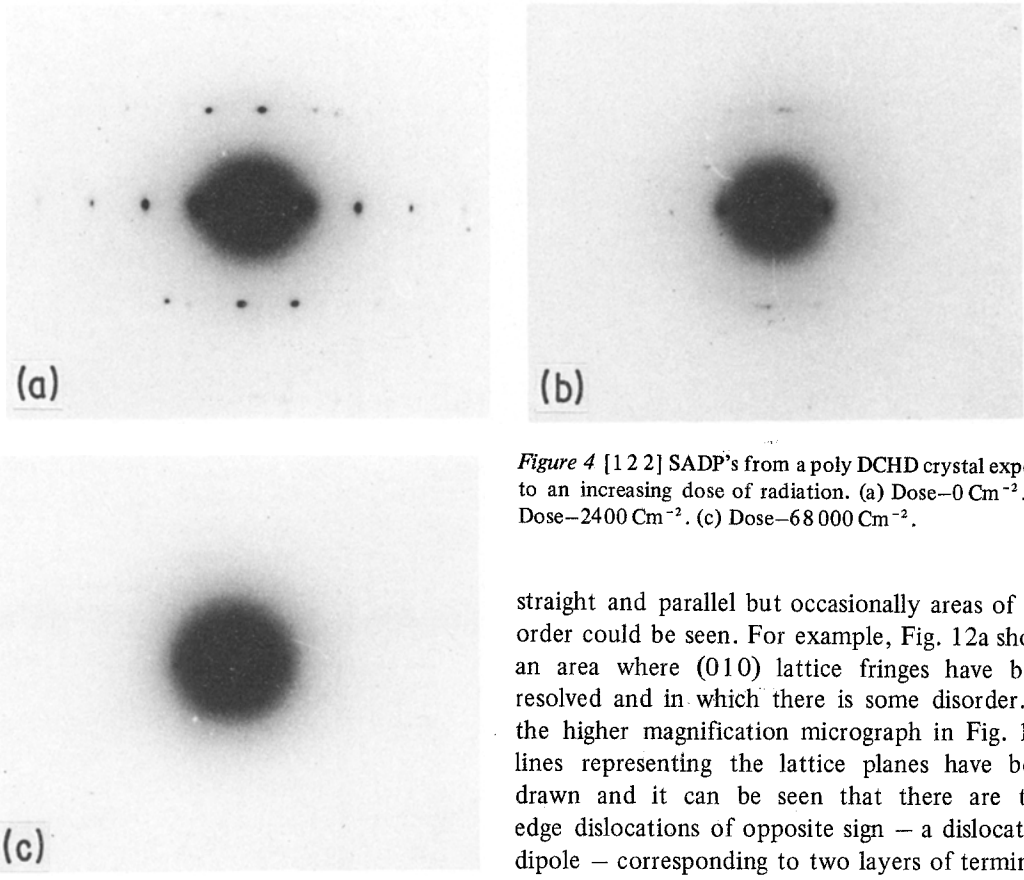

Figure 4 [1 2 2] SADP's from a poly DCHD crystal exposed to an increasing dose of radiation. (a) Dose–0 Cm^{-2}. (b) Dose–2400 Cm^{-2}. (c) Dose–68 000 Cm^{-2}.

In Fig. 10 particularly well-defined fringes are shown at a spacing of 1.1 ± 0.1 nm which corresponds to the spacing of $(1\bar{1}0)$ planes (1.17 nm) in the polymer. Finally Fig. 11 gives rather weak fringes at 0.9 ± 0.1 nm which corresponds to the spacing of (2 0 0), (1 1 0) or $(2\bar{1}0)$ planes (spacings 0.826, 0.862 and 0.813 nm, respectively) in poly DCHD.

In most cases the lattice fringes were very straight and parallel but occasionally areas of disorder could be seen. For example, Fig. 12a shows an area where (0 1 0) lattice fringes have been resolved and in which there is some disorder. In the higher magnification micrograph in Fig. 12b lines representing the lattice planes have been drawn and it can be seen that there are two edge dislocations of opposite sign – a dislocation dipole – corresponding to two layers of terminating molecules in the crystal.

4. Discussion

4.1. Radiation damage

Studies of radiation damage in the past have shown that the mechanisms of damage are different in different polymers. In general it is possible to divide them into two main groups, polymers which cross-link and polymers which degrade [15]. With electron beam damage it is rather difficult to make a quantitative assessment

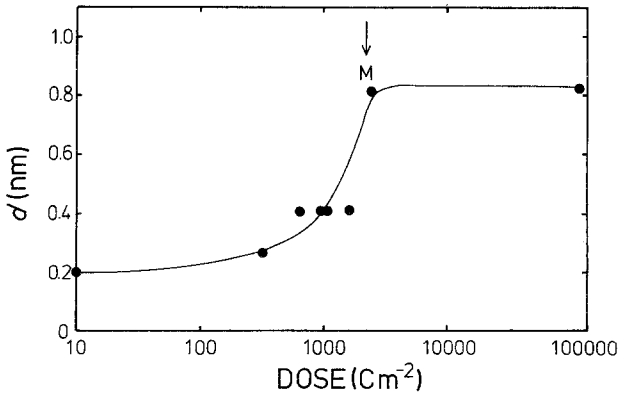

Figure 5 Dependence of *d*-spacings of fading diffraction spots upon radiation dose for poly DCHD. (The arrow indicates the dose required to obtain a micrograph).

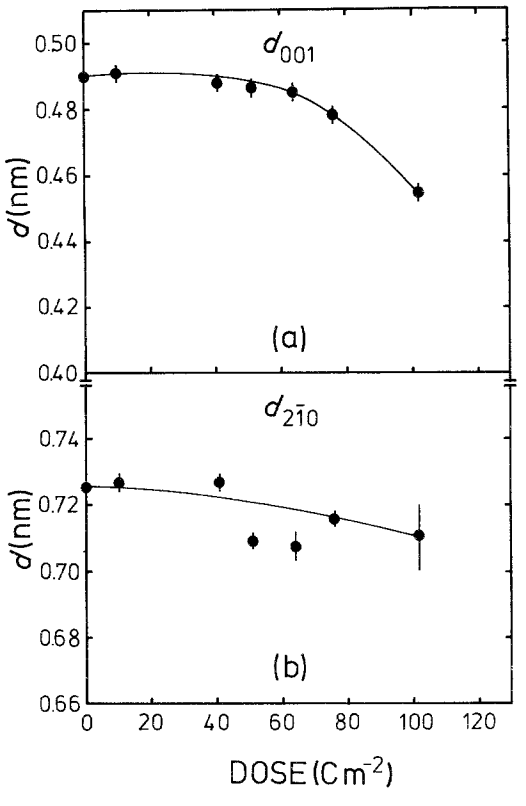

Figure 6 Variation in (0 0 1) and (2 $\bar{1}$ 0) *d*-spacings for poly TSHD with radiation dose.

as the irradiated samples are very small and difficult to characterize. However, the changes which occur during the irradiation process can be used to give an indication of the damage mechanisms. The main features of the damage in polydiacetylene crystals are as follows:

(a) The intensity of diffraction spots decreases gradually with spots corresponding to the lowest *d*-spacings disappearing first of all.

(b) The position of the spots changes but there is no significant broadening.

(c) Contrast is lost in bright and dark-field images but there appears to be no significant loss of material.

(d) Diffraction spots in poly TSHD fade fairly uniformly whereas (2 $\bar{1}$ 0) equatorial reflections are very persistent in poly DCHD.

The loss of diffraction spots clearly indicates a loss of crystalline order, initially short-range order and eventually longer-range order. The damaged polymer shows only diffuse rings corresponding to an amorphous structure. As there is no significant thinning or mass loss it would seem that the polymer undergoes cross-linking rather than chain scission [15]. The reduction in the *c*-repeat (Figs. 4 and 5) could be associated with cross-linking as in the case of polyethylene [15] where there is

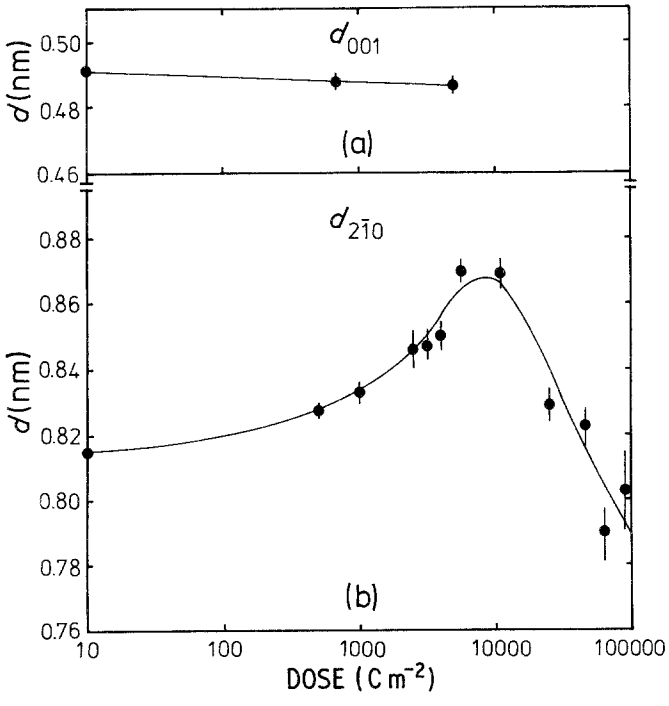

Figure 7 Variation in (0 0 1) and (2 $\bar{1}$ 0) *d*-spacings for poly DCHD with radiation dose.

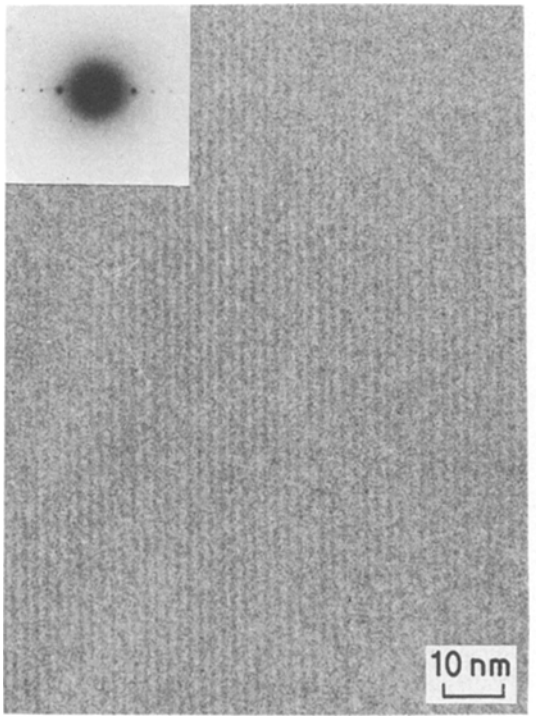

Figure 8 Lattice image from a poly DCHD crystal showing fringes with a spacing of 1.5 ± 0.1 nm. (Inset – SADP).

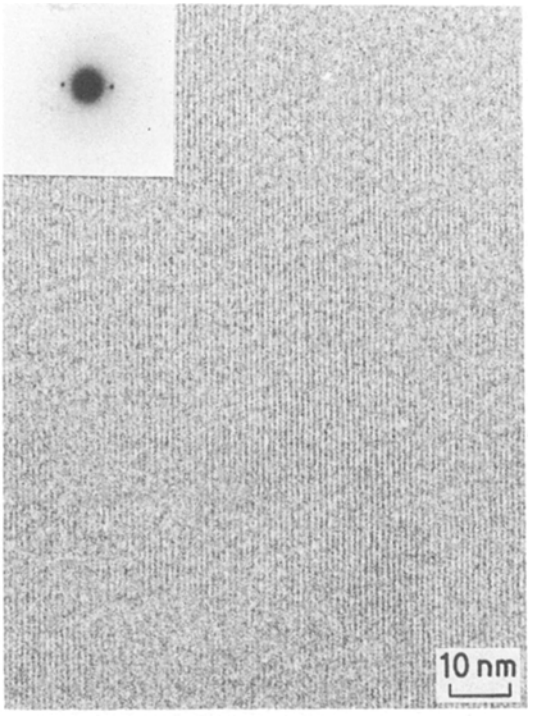

Figure 10 Lattice image from a poly DCHD crystal showing fringes with a spacing of 1.1 ± 0.1 nm. (Inset – SADP).

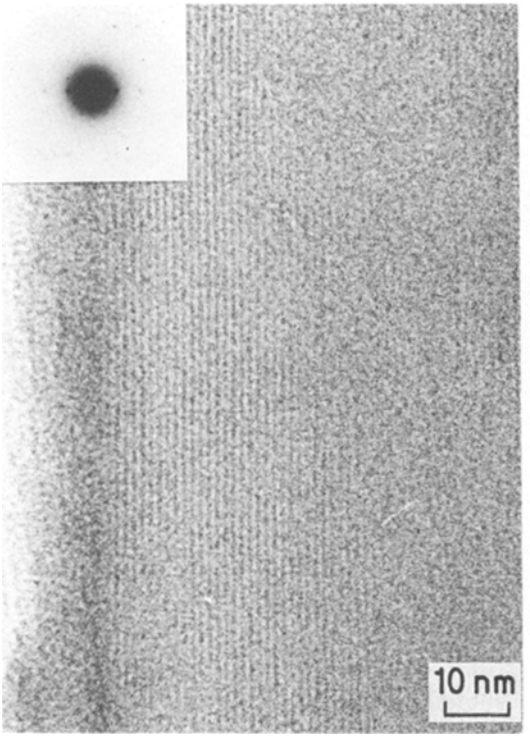

Figure 9 Lattice image from a poly DCHD crystal showing fringes with a spacing of 1.3 ± 0.1 nm. (Inset – SADP).

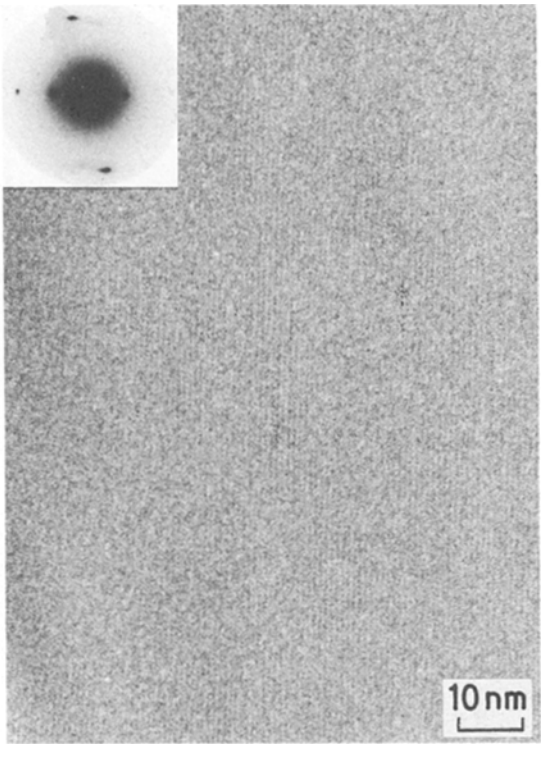

Figure 11 Lattice image from a poly DCHD crystal showing fringes with a spacing of 0.9 ± 0.1 nm. (Inset – SADP).

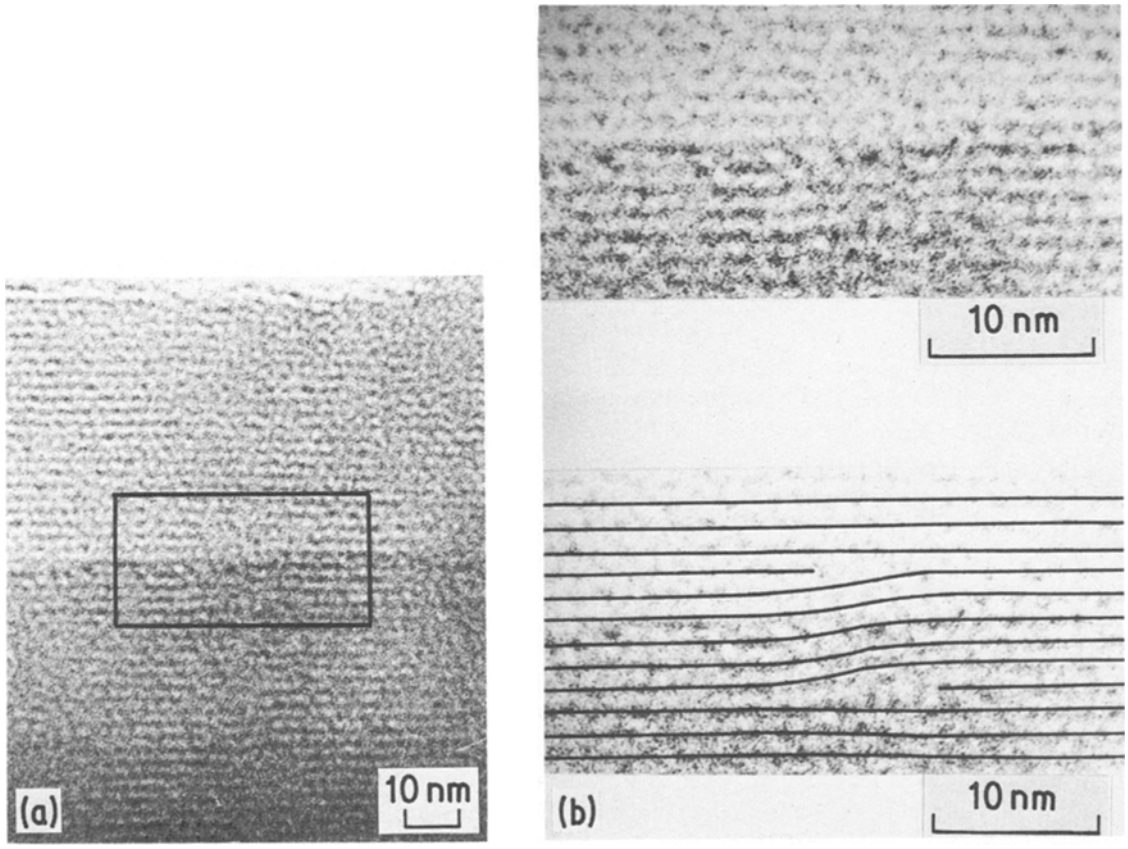

Figure 12 Lattice image from a poly DCHD crystal showing (0 1 0) fringes and containing defects. (a) Lattice image showing planes with 1.22 nm spacing. (b) Enlargements of rectangular area in (a) with the lattice planes sketched showing chain-end dislocation dipole.

considerable distortion of the crystal lattice during irradiation which causes cross-linking. The stabilization of the poly DCHD structure at high doses ($> 2500\,Cm^{-2}$) is particularly interesting with only a pair of strong equatorial $(2\,\bar{1}\,0)$ reflections remaining. Since only first-order spots and no higher order reflections remain it appears that the damaged structure is paracrystalline with a well-defined inter-chain spacing but with order parallel to the chain direction lost. As this does not happen with poly TSHD it would seem that this behaviour is related to the chemistry of the carbazole side groups in poly DCHD. The $(2\,\bar{1}\,0)$ planes are parallel to the plane of the zig-zag of the polymer backbone and also contain the side-groups [32]. Irradiation could cause cross-linking between side-groups in this plane to give a sheet structure which might then be stabilized against further damage. Another factor that may be significant is that poly DCHD has much better thermal stability than poly TSHD. Differential scanning calorimetry has shown that poly DCHD is stable up to at least 300° C whereas poly TSHD starts to undergo thermal degradation at 150° C.

Full details of the mechanisms of radiation damage will only be elucidated when bulk samples are irradiated. However, it is clear from Table II that poly DCHD is considerably more resistant to radiation damage by electrons than many other polymers. It should be pointed out that there are now a large number of different polydiacetylene derivatives available and this study has only concentrated upon two particular ones that were readily at hand. There may be other derivatives even more stable than poly DCHD and more knowledge of the mechanisms of radiation damage in polydiacetylenes should allow radiation stability to be optimized in these types of polymers.

4.2. High resolution microscopy of polymers

The main problem in applying HREM techniques

to polymers is radiation damage. Even if all the focusing is done adjacent to the area of interest, the area has to be irradiated in order to obtain a micrograph and the intensity of radiation will depend upon the magnification used and the sensitivity of the photographic film. The choice of magnification will depend upon the ability to resolve useful information from the background "noise" due to factors such as grain size of the film [16, 18]. It was found in this present study that it should be possible to resolve features of ~ 0.4 nm with Industrex CX film at a magnification of 100 000 times. At 100 kV this meant that in order to obtain an image on the film of reasonable intensity the area of interest on the specimen was subjected to a dose of ~ 2200 Cm^{-2}. This is similar to a value of ~ 2000 Cm^{-2} quoted by Tsuji *et al.* [14] for a different type of film at the same magnification using 500 kV electrons.

Once the minimum dose required to obtain an image is established it is necessary to determine how much damage the crystal will suffer while the image is being obtained, and hence if a high-resolution micrograph can be obtained. It is clear that some polymers in Table II, such as polyethylene and poly TSHD will undergo considerable damage before any images of the crystal lattice could be obtained. However, in all the polymers for which lattice images have been obtained, PPT [11], PBT [12], poly (*p*-xylylene) [14] and poly DCHD [13] the crystals are not fully damaged until a dose in excess of 2000 Cm^{-2} has been received. This is consistent with the amount of radiation required to obtain an image using fast film at a magnification of 100 000 times.

The doses given in Table II are mainly for "end-points" and the total loss of diffraction. Since the outer, high-angle, low *d*-spacing reflections fade first of all, there will be a gradual loss of resolution as the damage takes place. However, since resolution is limited to about 0.4 nm by instrumental factors such as the capabilities of the electron microscopes and film grain size, radiation damage may not control the maximum resolution that can be obtained. This will depend upon both the polymer and the experimental conditions used.

In this present study four distinct lattice images have been obtained, all from planes which are parallel to the chain direction, *c*. These are from high *d*-spacing (> 0.8 nm), low angle, $(h\,k\,0)$ planes and their equatorial reflections do not disappear until after the azimuthal reflections have faded, i.e. a dose of more than about 2500 Cm^{-2} has been received (Table II). It is clear that the stability of poly DCHD is sufficient to allow these lattice images to be obtained.

An important question arises as to whether or not it is possible to resolve the molecular structure as well as the lattice planes. Very recently, Tsuji and co-workers [14] have reported directly imaging the molecular chains in a poly (*p*-xylylene) lamellar single crystal. In these crystals the molecules are seen end-on and have an elliptical cross-section. The molecules in poly DCHD are oriented perpendicular to the electron beam and hence viewed side-ways. However, in order to achieve clear molecular definition it is essential that the molecules and side-groups are stacked parallel to the electron beam with their features superimposed as in the case of small organic molecules [7]. Because of the relatively complex structure of poly DCHD with 104 atoms per unit cell [32] it is not obvious in which beam directions, if any, the molecules will be stacked with their features superimposed. A computer simulation of the projected molecular structure in an electron micrograph at different levels of resolution in different viewing directions has been carried out [33]. Unfortunately, it appears that in poly DCHD the only direction in which the structure is superimposed is [0 0 1], i.e. parallel to the chain direction. Because of their chain-extended morphology poly DCHD crystals are all oriented with the beam approximately perpendicular to the chain direction. It was found that at the level of instrumental resolution being used (~ 0.4 nm) the only structures expected to be resolved strongly are lattice fringes parallel to the chain direction as found in practice. The structure factor for (0 0 1) reflections was found to be very low [33] and so it would not be expected that lattice images of (0 0 1) planes at a spacing of 0.491 nm and oriented perpendicular to the chain direction could be obtained, again as found in practice. The computation also allowed another issue to be settled. The lattice images of spacing 0.9 ± 0.1 nm could be from three possible planes, (2 0 0), (1 1 0) or $(2\,\bar{1}\,0)$ which have a similar spacing. It was found that of these three types of plane $(2\,\bar{1}\,0)$ had the highest structure factor and so it is highly likely that the 0.9 nm fringes in Fig. 11 are from $(2\,\bar{1}\,0)$ planes. Also the $(2\,\bar{1}\,0)$ reflections were found to be very persistent during radiation damage measurements, whereas the other reflections fade more quickly.

4.3. Defects in polymer crystals

Over the years there have been many suggestions of the types of defects present in polymer crystals [34–36]. So far, stacking faults [23] and dislocations with Burgers vectors parallel to the chain direction [24] have been reported. A dislocation which has been predicted theoretically [34] but not found until this present study is the edge dislocation with its Burgers vector perpendicular to the chain direction – a "chain-end" dislocation. The micrograph in Fig. 12b strongly indicates that these dislocations can exist in poly DCHD, probably in pairs of opposite sign dislocations, i.e. dipoles.

A question arises as to the origin of this dislocation. One possibility is that the feature is an artefact due to factors such as radiation damage. It is difficult to disprove this, although the damage may cause the dislocation dipole to form by chain rupture. Because the defect was difficult to find, it was the only one found on over 50 micrographs of lattice images, it is highly likely that it is not an artefact due to radiation damage. It also occurs at a step in the crystal when the thickness increases and the absorption contrast changes. Since crystal growth is known to occur through dislocations the dipole may have been formed during growth of the monomer crystal from solution. It could then have been "frozen-in" during solid-state polymerization. An alternative explanation is that the dipole could have formed during solid state polymerization which is thought to take place by the movement of radicals along the polymer backbone. The dislocations could be left by the decomposition of these radicals in the crystal.

5. Conclusions

It has been found that radiation damage in polydiacetylene single crystals in the electron microscope takes place by cross-linking rather than degradation and the rate at which it occurs depends upon the structure of the polydiacetylene. It was found that the derivative, poly DCHD, was sufficiently resistant to damage to allow at least four different lattice images to be obtained. Unfortunately, the molecules in poly DCHD do not stack in the crystals such that their features are superimposed so it has not been possible to resolve the shape of individual molecules in the crystals. However, it has been possible for the first time to directly observe contrast from a chain-end dislocation dipole.

Acknowledgements

This work was supported by the Science and Engineering Research Council. The authors would like to thank Mr I. Chalmers for synthesis of the DCHD monomer and Dr D. Bloor for his help and valuable discussion. They are also grateful to Dr J. R. Fryer for use of the 100 C microscope in Glasgow and for his advice. Finally they would like to thank Dr C. J. Humphreys and Dr J. Anstis of the University of Oxford for help with image simulation.

References

1. G. VAN TENDELOO, *J. Microsc.* **119** (1980) 125.
2. N. W. JEPPS and T. F. PAGE, *ibid.* **119** (1980) 177.
3. L. A. BURSILL and G. J. WOOD, *Phil. Mag.* **A38** (1978) 673.
4. V. E. COSSLETT, R. A. CAMPS, W. O. SAXTON, D. T. SMITH, W. C. NIXON, H. AHMED, C. J. D. CATTO, J. R. A. CLEAVER, K. C. A. SMITH, A. E. TIMBS, P. W. TURNER and P. M. ROSS, *Nature* **281** (1979) 49.
5. Y. MURATA, J. R. FRYER and T. BAIRD, *J. Microsc.* **108** (1976) 261.
6. Y. MURATA, J. R. FRYER, T. BAIRD and H. MURATA, *Acta Crystallogr.* **A33** (1977) 198.
7. J. R. FRYER, *ibid.* **A34** (1978) 603.
8. J. R. FRYER, *J. Microsc.* **120** (1980) 1.
9. D. J. SMITH and J. R. FRYER, *Nature* **291** (1981) 481.
10. A. KELLER, *Koll. Z.u.Z. Polym.* **231** (1969) 386.
11. M. G. DOBB, D. J. JOHNSON and B. P. SAVILLE, *J. Polym. Sci. Polym. Symp.* **58** (1977) 237.
12. K. SHIMAMURA, J. R. MINTER and E. L. THOMAS, *J. Mater. Sci. Lett.* **2** (1983) 54.
13. R. T. READ and R. J. YOUNG, *J. Mater. Sci.* **16** (1981) 2922.
14. M. TSUJI, S. ISODA, M. OHARA, A. KAWAGUCHI and K. KATAYAMA, *Polymer* **23** (1982) 1568.
15. D. T. GRUBB, *J. Mater. Sci.* **9** (1974) 1715.
16. R. M. GLAESER in "Physical Aspects of Electron Microscopy and Microbeam Analysis", edited by B. M. Siegel and D. R. Beaman (Wiley, New York, 1975).
17. E. ZEITLER, EMAG 1981, *Inst. Phys. Conf. Ser.* **61** (*Inst. Phys., London, 1981*).
18. W. JONES, in "Surface and Defect Properties of Solids" (*Chem. Soc. Spec. Period. Rep.*) **5** (1976) 65.
19. D. J. GRUBB and G. W. GROVES, *Phil. Mag.* **24** (1971) 815.
20. L. E. THOMAS, C. J. HUMPHREYS, W. R. DUFF and D. T. GRUBB, *Radiation Effects* **3** (1970) 89.
21. J. R. FRYER, *Proc. Roy. Microsc. Soc.* **17** (1982) 578.
22. N. UYEDA, J. KOBOYASHI, K. ISHIZUKA and Y. FUJIYOSHI, *Chem. Scripta* **14** (1979) 47.
23. R. J. YOUNG, R. T. READ and J. PETERMANN, *J. Mater. Sci.* **16** (1981) 1835.
24. R. J. YOUNG and J. PETERMANN, *J. Polym. Sci. Polym. Phys. Ed.* **20** (1982) 961.

25. G. WEGNER, *Z. Naturforsch.* **24b** (1969) 824.
26. K. C. YEE and R. R. CHANCE, *J. Polym. Sci. Polym. Phys. Ed.* **16** (1978) 431.
27. A. FALLS and E. L. THOMAS, University of Massachussetts, private communication (1981).
28. J. C. H. SPENCE, "Experimental High Resolution Electron Microscopy" (Oxford University Press, Oxford, 1980).
29. J. W. EDINGTON, "Monographs in Practical Electron Microscopy in Materials Science" **1** (MacMillan, London, 1974).
30. R. C. WILLIAMS and H. W. FISHER, *J. Mol. Biol.* **52** (1970) 121.
31. D. KOBELT and E. F. PAULUS, *Acta Crystallogr.* **B30** (1974) 232.
32. V. K. ENKELMANN, R. J. LEYRER, G. SCHLEIER and G. WEGNER, *J. Mater. Sci.* **15** (1980) 168.
33. J. ANSTIS and C. J. HUMPHREYS, University of Oxford, private communication (1982).
34. P. PREDECKI and W. O. STATTON, *J. Appl. Phys.* **37** (1966) 4053.
35. J. M. PETERSON, *ibid.* **37** (1966) 4047.
36. R. J. YOUNG, *Phil. Mag.* **30** (1974) 85.

Received 22 April
and accepted 26 May 1983